

Potential Impact of Biofield Energy Treatment on the Atomic, Physical and Thermal Properties Indium Powder

Trivedi MK¹, Tallapragada RM¹, Branton A¹, Trivedi D¹, Nayak G¹, Latiyal O² and Jana S^{2*}

¹Trivedi Global Inc., 10624 S Eastern Avenue Suite A-969, Henderson, NV 89052, USA

²Trivedi Science Research Laboratory Pvt. Ltd., Hall-A, Chinar Mega Mall, Chinar Fortune City, Hoshangabad Rd., Bhopal- 462026, Madhya Pradesh, India

Abstract

Indium has gained significant attention in the semiconductor industries due to its unique thermal and optical properties. The objective of this research was to investigate the influence of the biofield energy treatment on the atomic, physical and thermal properties of the indium. The study was performed in two groups (control and treated). The control group remained as untreated, and treated group received Mr. Trivedi's biofield energy treatment. Subsequently, the control and treated indium samples were characterized by the X-ray diffraction (XRD), Differential scanning calorimetry (DSC), Thermogravimetric analysis (TGA), and Fourier transform infrared (FT-IR) spectroscopy. The XRD diffractogram showed the shifting of peaks toward higher Bragg's angles in the treated indium sample as compared to the control. The crystallite size of treated indium sample were substantially changed from -80% to 150.2% after biofield energy treatment, as compared to control. In addition, the biofield energy treatment has altered the lattice parameter (-0.56%), unit cell volume (-0.23%), density (0.23%), atomic weight (-0.23), and nuclear charge per unit volume (1.69%) of the treated indium sample with respect to the control. The DSC showed an increase in the latent heat of fusion up to 3.23% in the treated indium sample with respect to control. Overall, results suggest that biofield energy treatment has substantially altered the atomic, physical, and thermal properties of treated indium powder. Therefore, the treated indium could be utilized in thermal interface material in semiconductor industries.

Keywords: Indium; Biofield energy treatment; X-Ray Diffraction; Differential Scanning Calorimetry; Thermogravimetric Analysis; Fourier Transform Infrared Spectroscopy

Introduction

Indium (In), a post transition metallic element, is soft, malleable and easily fusible metal. Indium is utilized in various low melting point alloys like soft metal, solder, and galinstan [1]. It is the primary source for the production of the indium tin oxide that is used in transparent conductive coating on the glass. Indium is produced from the residue, which generated during zinc ore processing. In addition, it is also present in the iron, lead and copper ores [2]. Globally, around 50% of indium is consumed in the manufacturing of LCD (Liquid crystal displays) for computer monitors and televisions [3,4]. In semiconductor industries, it is used in the production of indium antimonide, indium phosphide, and indium nitride. Furthermore, indium is used in personal computers as thermal interface material (TIM), which is fitted between microprocessor and heat sink due to its excellent thermal conductivity [5]. In TIM, the thermal conductivity, melting point, and the latent heat of fusion play a crucial role [6,7]. Based on current rates of extraction, there are fewer than 14 years left of indium supplies. Currently, recycling is the only method to enhance the life span of indium in the industries [8]. Thus, it is important to enhance the efficiency of the indium for industrial applications. Hence, after considering the industrial application of indium, authors wish to investigate the impact of biofield energy treatment on atomic, physical, and thermal properties of indium.

The presence of electromagnetic field around the human body is evidenced by various medical technologies such as electromyography, electrocardiography, and the electroencephalogram [9]. It is demonstrated that bioelectricity is generated from the heart, brain functions or due to the motion of charged particles such as protons, electrons, and ions in the human body and form the electric field [10]. Further, due to the motion of charge particles, a magnetic field is generated, which is cumulatively known as the electromagnetic field. Thus, the electromagnetic field, which surrounds the human body

is called biofield. Therefore, a human has the ability to harness the energy from environment/Universe and can transmit it to any object (living or non-living) around the Globe. The object(s) always receive the energy and respond into a useful way that is called biofield energy, and this process is known as biofield energy treatment. The National center for Complementary and alternative medicine (NCCAM) has recommended uses of alternative CAM therapies in the healthcare sector [11]. CAM include numerous energy-healing therapies, and biofield therapy, is one of the energy medicine widely used worldwide to improve the health. Mr. Trivedi's unique biofield energy treatment (The Trivedi Effect®) is known to alter the atomic, structural, and physical characteristics of various metals [12,13] and ceramics [14,15]. The biofield energy treatment has shown excellent results in improving the antimicrobial susceptibility pattern, and alteration of biochemical reactions, as well as induced alterations in characteristics of pathogenic microbes [16,17]. The biofield energy treatment has significantly altered the melting point and latent heat of fusion in lead and tin powder [18]. In addition, Ye reported that the high energy treatment had significantly altered the microstructure and mechanical properties of titanium alloys [19,20]. Recently, our group reported that biofield treatment has altered the bond length of Ti-O in barium titanate [21] and reduced the crystallite size by 28.6% in magnesium powder [22]. Hence, based on excellent outcomes with biofield energy treatment on

*Corresponding author: Jana S, Trivedi Science Research Laboratory Pvt. Ltd., Hall-A, Chinar Mega Mall, Chinar Fortune City, Hoshangabad Rd., Bhopal- 462026, Madhya Pradesh, India, Tel : 917556660006; E-mail: publication@trivedisrl.com

Received September 02, 2015; Accepted September 09, 2015; Published September 19, 2015

Citation: Trivedi MK, Tallapragada RM, Branton A, Trivedi D, Nayak G, et al. (2015) Potential Impact of Biofield Energy Treatment on the Atomic, Physical and Thermal Properties Indium Powder. J Material Sci Eng 4: 198. doi:10.4172/2169-0022.1000198

Copyright: © 2015 Trivedi MK, et al. This is an open-access article distributed under the terms of the Creative Commons Attribution License, which permits unrestricted use, distribution, and reproduction in any medium, provided the original author and source are credited.

metals and ceramics, this work was undertaken to evaluate the impact of this on the atomic, physical, and thermal properties of the indium using x-ray diffraction (XRD), differential scanning calorimetry (DSC), thermogravimetric analysis (TGA), and Fourier transform infrared (FT-IR) spectroscopy.

Materials and Methods

Indium was procured from Alfa Aesar. The sample was divided into two parts; one was kept as a control sample while the other was subjected to Mr. Trivedi's unique biofield treatment and coded as treated sample. The treated group was in sealed pack and handed over to Mr. Trivedi for biofield treatment under laboratory condition. Mr. Trivedi provided the treatment through his energy transmission process to the treated group without touching the sample. The control and treated samples were characterized by using XRD, DSC, TGA, and FT-IR techniques.

XRD study

XRD analysis of control and treated indium was performed on Phillips, Holland PW 1710 X-ray diffractometer system, which had a copper anode with nickel filter. The radiation of wavelength used by the XRD system was 1.54056 Å. The data obtained from this XRD were in the form of a chart of 2θ vs. intensity and a detailed table containing peak intensity counts, d value (Å), full width half maximum (FWHM) (θ°), relative intensity (%) etc. The crystallite size (G) was calculated by using formula:

$$G = k\lambda / (b \cos\theta)$$

Here, λ is the wavelength of radiation used, b is FWHM of peaks and k is the equipment constant (=0.94). Percentage change in crystallite size was calculated using following formula:

$$\text{Percentage change in crystallite size} = [(G_t - G_c) / G_c] \times 100$$

Where, G_c and G_t are crystallite size of control and treated powder samples respectively.

Further, crystal structure parameters such as lattice parameter, unit cell volume of control and treated were computed using PowderX software.

Thermal analysis

The thermal analysis of indium powder was performed using DSC and TGA-DTA. The DSC was used to investigate the melting temperature and latent heat of fusion (ΔH) of samples. The control and treated indium samples were analyzed using a Pyris-6 Perkin Elmer DSC at a heating rate of 10°C/min under air atmosphere and the air was flushed at a flow rate of 5 mL/min. Predetermined amount of sample was kept in an aluminum pan and closed with a lid. A blank aluminum pan was used as a reference. Percentage change in latent heat of fusion was calculated using following equations:

$$\% \text{ change in Latent heat of fusion} = \frac{[\Delta H_{\text{Treated}} - \Delta H_{\text{Control}}]}{\Delta H_{\text{Control}}} \times 100$$

Where, $\Delta H_{\text{Control}}$ and $\Delta H_{\text{Treated}}$ are the latent heat of fusion of control and treated samples, respectively. For TGA-DTA analysis, Mettler Toledo simultaneous TGA-DTA was used to analyze the thermal characteristics of indium powder. The samples were heated from room temperature to 400°C with a heating rate of 5°C/min under air atmosphere.

FT-IR spectroscopy

FT-IR spectra were recorded on Shimadzu's Fourier transform infrared spectrometer (Japan) with frequency range of 4000-500 cm^{-1} . The analysis was accomplished to evaluate the effect of biofield treatment on dipole moment, force constant and bond strength in chemical structure [23].

Results and Discussion

XRD study

XRD diffractogram of control and treated indium samples is shown in Figure 1. XRD diffractogram of control sample showed crystalline peaks at 2θ equal to 32.95°, 36.29°, 39.15°, 54.44°, 56.58°, 63.21°, 67.04°, and 69.11°. The 2θ values found in control XRD pattern were similar to standard values, which were reported in literature [24]. However, XRD of treated sample showed intense peaks at 2θ equal to 33.08°, 36.44°, 39.29°, 54.60°, 56.73°, 63.33°, 67.19°, 69.24°, and 84.20°. This data suggests that XRD peaks were shifted toward higher angles in treated sample as compared to control, after biofield treatment. Moreover, the shifting of all XRD peaks toward higher angles suggested that lattice parameter of unit cell was decreased in treated indium powder as compared to the control. It was already reported that reduction in lattice parameter and unit cell volume lead to shift the XRD peaks toward higher angles [25]. Based on XRD peaks, control and treated samples were indexed with tetragonal crystal structure. The index planes corresponding to all XRD peaks and their respective crystallite size of control and treated indium samples are presented in Table 1. The data showed that the crystallite sizes were same in control and treated samples along plane (101), (002), and (103) as 107.9 nm, 217.8 nm, and 243.2 nm respectively. However, the crystallite sizes along planes (110), (200), (211), and (202) were significantly reduced from 109.8→87.9 nm, 235.1→156.8 nm, 165.6→33.1 nm, and 251.5→167.8 nm in treated indium sample. This indicates that crystallite sizes in treated indium were significantly reduced by 20, 33.3, 80, and 33.3% along planes (110), (200), (211), and (202), respectively as compared to control. Contrarily, the crystallite size was significantly increased by 150.2% (93.1 →232.9 nm) along plane (112) in the treated indium sample as compared to control (Figure 2). In addition, it was also observed that the relative intensities of all peaks with respect to (101) plane were significantly altered in treated indium powder as compared to control. The data showed that the relative intensities of peaks corresponding to (002), (110), (112), (200), (103), (211), and (202) planes were altered as 11→51.2, 21.1→47.1, 6.5→26.1, 21.6 →16.1, 23.5→13.9, 35.6→5.8, and 4.4→9.4 respectively. Inoue reported that the change in crystal morphology leads to alter the relative intensities of XRD peaks [26]. Recently, our group reported that biofield treatment has altered the particle size, surface area, and surface morphology in aluminium [13], lead [18] and antimony sulfide [27]. Thus, it is assumed that the biofield treatment, possibly altered the surface morphology of indium powder, which may alter the relative intensities in treated sample as compared to control. The XRD data of the control and treated samples were analyzed using Powder X software and various parameters such as lattice parameter, unit cell volume, density, atomic weight and nuclear charge per unit volume were computed, which are presented in Table 2. The data exhibited that the lattice parameter and unit cell volume of treated indium powder were reduced by 0.56 and 0.23%, respectively, as compared to control. The reduction in lattice parameter and unit cell volume was corroborated by shifting of XRD peaks toward higher angles. Kumar reported that the XRD peaks can shift to higher side if larger radii atoms are replaced by smaller radii atoms [28]. Due to

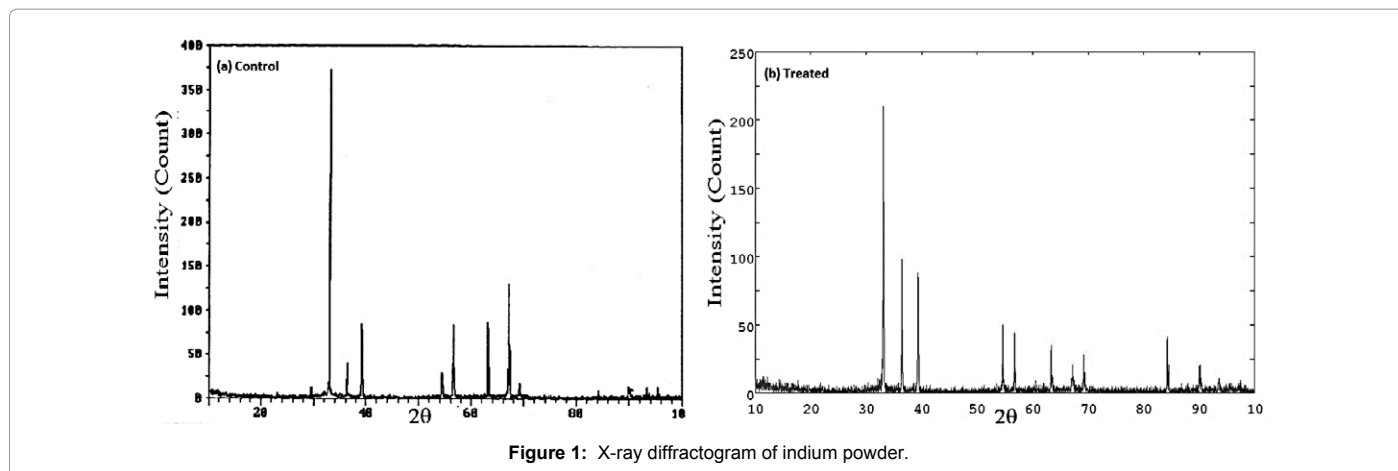


Figure 1: X-ray diffractogram of indium powder.

Standard		Control				Treated (T1)			
2 θ (degree)	Plane (hkl)	2 θ (degree)	Relative Intensity	FWHM (degree)	Crystallite size (nm)	2 θ (degree)	Relative Intensity	FWHM (degree)	Crystallite size (nm)
32.965	101	32.95	100	0.1	107.9	33.08	100	0.1	107.9
36.32	2	36.29	11	0.06	217.8	36.44	51.2	0.06	217.8
39.17	110	39.15	21.1	0.1	109.8	39.29	47.1	0.12	87.9
54.47	112	54.44	6.5	0.12	93.1	54.6	26.1	0.06	232.9
56.56	200	56.58	21.6	0.06	235.1	56.73	16.1	0.08	156.8
63.204	103	63.21	23.5	0.06	243.2	63.33	13.9	0.06	243.2
67.034	211	67.04	35.6	0.08	165.6	67.19	5.8	0.32	33.1
69.115	202	69.11	4.4	0.06	251.5	69.24	9.4	0.08	167.8

Table 1: Effect of biofield energy treatment on relative peak intensity, Bragg's angle, and crystallite size of indium powder.

Group	Lattice parameter (Å)	Unit cell volume ($\times 10^{-23} \text{ cm}^3$)	Density (g/cc)	Atomic weight (g/mol)	Nuclear charge per unit volume (C/m^3)
Control	3.250	5.2280	7.36745	115.993	436233
Treated (T1)	3.231	5.2161	7.38425	115.729	443612
Percent Change	-0.56	-0.23	0.23	-0.23	1.69

Table 2: Effect of biofield energy treatment on lattice parameter, unit cell volume density atomic weight, nuclear charge per unit volume of indium powder.

indium powder. Moreover, the reduction in lattice parameter of unit cell led to the increase in density of treated indium powder by 0.23% as compared to control. The atomic weight of treated indium powder was reduced by 0.23% as compared to control. In addition, the nuclear charge per unit volume of treated indium was increased by 1.69% as compared to control. Based on the alteration in nuclear charge per unit volume and atomic weight, it is hypothesized that the biofield energy treatment might induce reversible nuclear level reactions, which may alter the number of protons and neutrons in indium nuclei. It might be the reason for alteration of atomic weight and nuclear charge per unit volume in treated indium powder.

Thermal analysis

The DSC thermogram of control and treated samples are presented in Figures 3a-3d. DSC thermogram of control indium showed an endothermic sharp inflection at 159.94°C due to melting temperature of the sample. However, this melting temperature was reduced to 157.61°C, 157.72°C, and 157.50°C in treated T1, T2 and T3 samples, respectively. It indicated that melting temperature was decreased by 1.45, 1.38, 1.52% in the treated indium samples T1, T2, and T3 respectively, as compared to control. Further, the sharp melting peaks in control and treated samples suggested the crystalline nature of indium samples. Fundamentally, melting point is related to thermal vibrations of atoms in a solid. Levitas reported that the stress, induced by transformation strain leads to increase the driving force for melting and reduces the melting temperature [29]. The existence of internal strain and stress is evidenced by shifting of XRD peaks in treated indium to higher Bragg angle, after biofield treatment. Thus, it is assumed that the energy, which probably transferred through biofield treatment, might induce internal strain in treated indium powder. Due

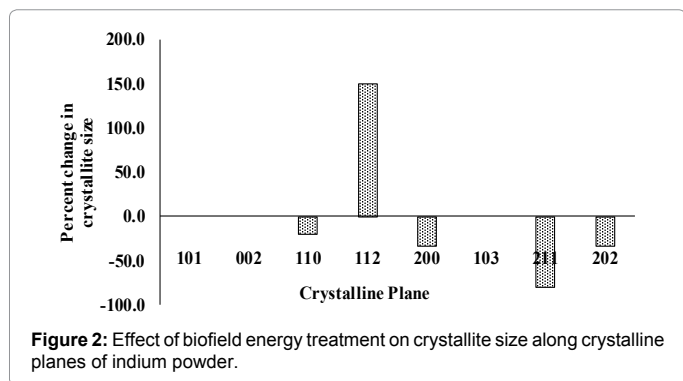
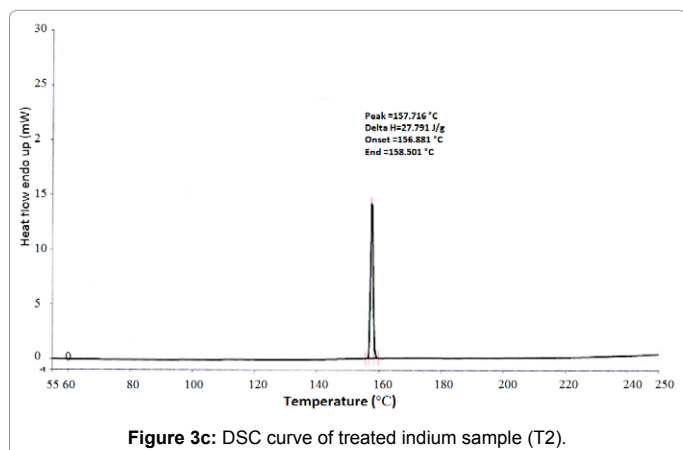
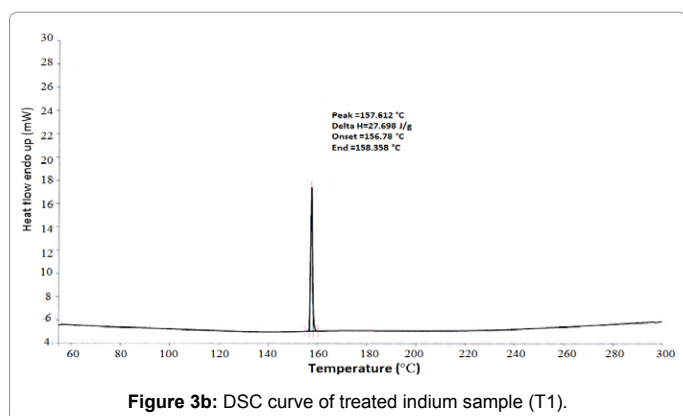
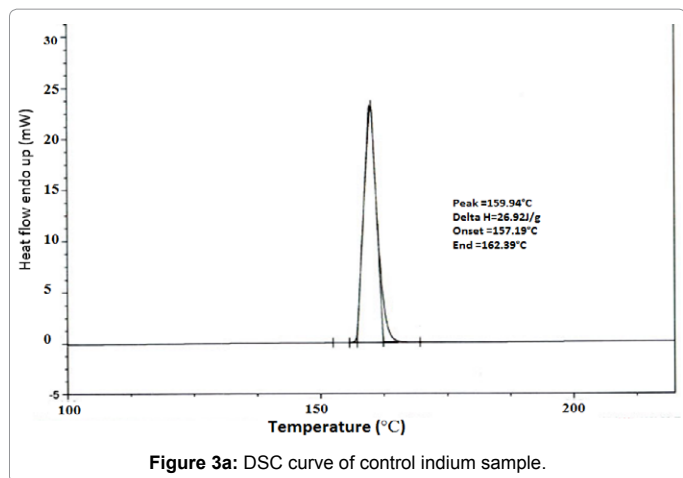


Figure 2: Effect of biofield energy treatment on crystallite size along crystalline planes of indium powder.

substitution of small radii atoms, the lattice constant of unit cell decrease and that results into higher Bragg's angle. Thus, based on shifting of XRD peaks and reduction in the lattice parameter, it is assumed that biofield treatment might induce compressive stress in treated indium powder and that might be responsible for internal strain in treated

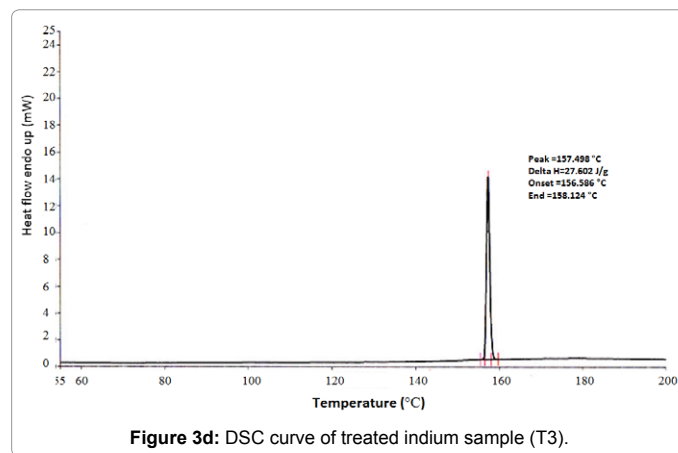


to this, the melting point possibly decreased in treated indium powder after biofield treatment. The latent heat of fusion was obtained from the respective thermogram of control and treated indium and data are presented in Table 3. The control indium showed a latent heat of fusion of 26.92 J/g and it was increased to 27.70, 27.79, and 27.60 J/g in the treated samples T1, T2 and T3, respectively. The result showed 2.89%, 3.23%, and 2.52% increase in latent heat of fusion in treated indium samples T1, T2 and T3, respectively, as compared to control. The latent heat of fusion is the energy required by the material to overcome the interatomic interaction to change the phase from solid to liquid. The reduction found in lattice parameter of treated indium suggests that the distance between atoms decreased after biofield treatment. It is

reported that decrease in interatomic distance leads to increase the interatomic interaction [30]. Moreover, it is well demonstrated that latent heat of fusion of solids increases with increase in interatomic interaction [31,32]. Thus, it is assumed that the interatomic interaction of indium atoms probably enhanced after biofield treatment and that might be responsible for higher latent heat of fusion in treated samples as compared to control. TGA-DTA analysis results of control and treated indium sample are presented in Table 4. The DTA result showed the endothermic peak at 155.94°C, 156.11°C, and 156.23°C in control, T1 and T4 respectively. The thermal energy involved in this process was 26.83, 27.44, and 25.64 J/g in control, T1 and T4 samples, respectively. Further, TGA data showed the percent change in weight control, T1, and T4 *i.e.* -9.04, -3.31, and 3.07% respectively. Thus, overall data indicates that biofield treatment has altered the thermal properties of indium powder. The alteration of melting point and latent heat of fusion in treated indium could play an important role in thermal interface material (TIM) applications in semiconductor industries.

FT-IR spectroscopy

FT-IR spectra of the control and treated indium samples are presented in Figure 4. FT-IR spectra showed absorption peak at 3768 and 3730 cm^{-1} in control and treated indium sample, which could be due to O-H stretching vibration. The absorption peak found at 3028 and 2997 cm^{-1} in control and treated indium sample respectively, due to CO_2 absorption from atmosphere. In addition, the absorption peaks observed in control sample at 569 and 416 cm^{-1} attributing to indium-oxide bonding vibrations were changed to 565 and 435 cm^{-1} in



Parameter	Control	T1	T2	T3
Melting Temperature (°C)	159.94	157.61	157.72	157.50
Percent change in melting temperature	-	-1.45	-1.38	-1.52
Latent heat of fusion, ΔH (J/g)	26.92	27.70	27.79	27.60
Percent change in ΔH	-	2.89	3.23	2.52

Table 3: Differential scanning calorimetry (DSC) analysis of control and treated of Indium powder samples.

Parameter	Control	T1	T4
DTA integral area (s°C)	18.13	16.69	11.64
Peak temperature (°C)	155.94	156.11	156.23
Heat of reaction, ΔH (J/g)	26.83	27.44	25.64
Percent weight loss	-9.041	-3.31	3.07

T1, T4 are treated samples

Table 4: TGA-DTA analysis of control and treated of indium powder.

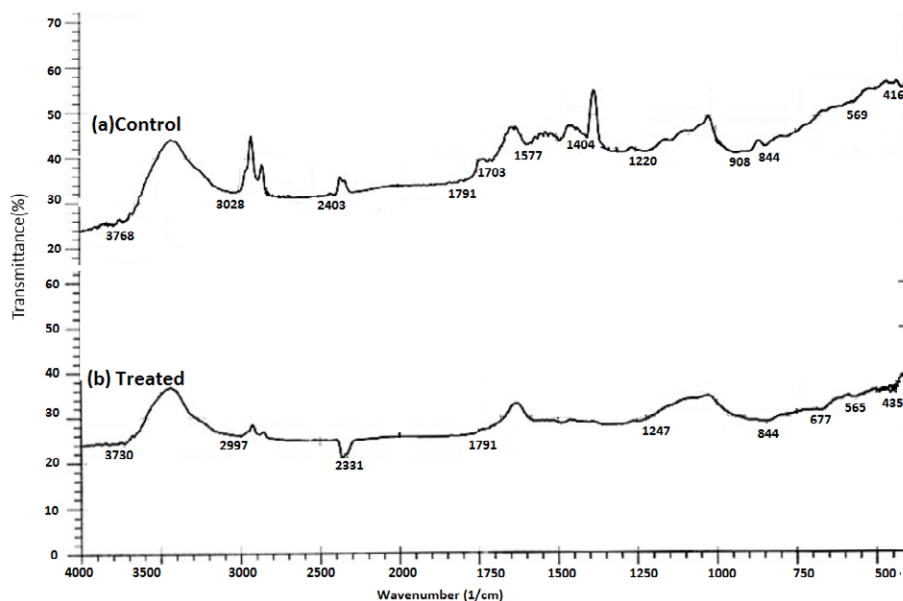


Figure 4: FT-IR spectra of indium powder.

treated sample [33]. Overall, the FT-IR results showed an alteration in bonding properties in indium powder.

Conclusion

The XRD analysis showed that the alteration in crystallite size from -80% to 150.2% in the treated indium as compared to control. The lattice parameter, unit cell volume, density, atomic weight, and nuclear charge per unit volume of the treated powder were altered after biofield treatment. In addition, a significant alteration in relative intensities of all XRD peaks suggested the modification in crystal morphology of treated indium after biofield energy treatment. Besides, the thermal analysis results indicated the increase in latent heat of fusion (upto 3.23%), which could be due to increase in interatomic attractive force in treated sample. Overall, the result demonstrated that Mr. Trivedi's biofield energy treatment could be applied to modify the thermal and physical properties of indium for semiconductor industries.

Acknowledgement

Authors thank Dr. Cheng Dong of NLSC, Institute of Physics, and Chinese academy of sciences for permitting us to use Powder-X software for analyzing XRD results. The authors would also like to thank Trivedi Science, Trivedi Master Wellness and Trivedi Testimonials for their support during the work.

References

1. Surmann P, Zeyat H (2005) Voltammetric analysis using a self-renewable non-mercury electrode. *Anal Bioanal Chem* 383: 1009-1013.
2. Alfantazi AM, Moskalyk RR (2003) Processing of indium: A review. *Miner Eng* 16: 687-694.
3. Bhuiyan AG, Hashimoto A, Yamamoto A (2003) Indium nitride (InN): A review on growth, characterization, and properties. *J Appl Phys* 94: 2779.
4. Bachmann KJ (1981) Properties, preparation, and device applications of indium phosphide. *Annu Rev Mater Sci* 11: 441-484.
5. Tong XC (2011) *Advanced Materials for Thermal Management of Electronic Packaging*. Springer.
6. Too SS, Touzelbaev M, Khan M, Master R, Diep J, et al. (2009) Indium thermal interface material development for microprocessors. *Proc 25th Annu IEEE SEMI-THERM* 186 -192.
7. Yu JK, Kang SG, Jung KC, Han JS, Kim DH (2007) Fabrication of nano-sized ITO powder from waste ITO target by spray pyrolysis process. *Mater Trans* 48: 249-257.
8. Choi D, Hong SJ, Son Y (2014) Characteristics of indium tin oxide (ITO) nanoparticles recovered by lift-off method from TFT-LCD panel scraps. *Materials* 7: 7662-7669.
9. Zahra M, Farsi M (2009) Biofield therapies: Biophysical basis and biological regulations. *Complement Ther Clin Pract* 15: 35-37.
10. Neuman MR (2000) *Biopotential electrodes: The biomedical engg handbook*. (2nd edn) CRC Press LLC, Boca Raton.
11. Barnes PM, Powell-Griner E, McFann K, Nahin RL (2004) *Complementary and alternative medicine use among adults: United States, 2002*. *Adv Data* 343: 1-19.
12. Trivedi MK, Tallapragada RM (2008) A transcendental to changing metal powder characteristics. *Met Powder Rep* 63: 22-28, 31.
13. Trivedi MK, Patil S, Tallapragada RMR (2015) Effect of biofield treatment on the physical and thermal characteristics of aluminium powders. *Ind Eng Manag* 4: 151.
14. Trivedi MK, Nayak G, Patil S, Tallapragada RM, Latiyal O (2015) Studies of the atomic and crystalline characteristics of ceramic oxide nano powders after bio field treatment. *Ind Eng Manag* 4: 161.
15. Trivedi MK, Patil S, Tallapragada RM (2013) Effect of biofield treatment on the physical and thermal characteristics of vanadium pentoxide powder. *J Material Sci Eng S11*: 001.
16. Trivedi MK, Patil S, Shettigar H, Gangwar M, Jana S (2015) Antimicrobial sensitivity pattern of *Pseudomonas fluorescens* after biofield treatment. *J Infect Dis Ther* 3: 222.
17. Trivedi MK, Patil S, Shettigar H, Bairwa K, Jana S (2015) Phenotypic and biotypic characterization of *Klebsiella oxytoca*: An impact of biofield treatment. *J Microb Biochem Technol* 7: 203-206.
18. Trivedi MK, Patil S, Tallapragada RM (2013) Effect of biofield treatment on the physical and thermal characteristics of silicon, tin and lead powders. *J Material Sci Eng* 2: 125.
19. Ye X, Tse ZTH, Tang G, Song G (2014) Effect of electroplastic rolling on deformability, mechanical property and microstructure evolution of Ti-6Al-4V alloy strip. *Mater Charact* 98: 147-161.
20. Ye X, Tse ZTH, Tang G, Geng Y, Song G (2015) Influence of electropulsing globularization on the microstructure and mechanical properties of Ti-6Al-4V alloy strip with lamellar microstructure. *Mater Sci Eng A* 622: 1-6.

21. Trivedi MK, Nayak G, Patil S, Tallapragada RM, Latiyal O, et al. (2015) Impact of biofield treatment on atomic and structural characteristics of barium titanate powder. Ind Eng Manage 4: 166.
22. Trivedi MK, Tallapragada RM, Branton A, Trivedi D, Nayak G, et al. (2015) Potential impact of biofield treatment on atomic and physical characteristics of magnesium. Vitam Miner 3: 129.
23. Pavia DL, Lampman GM, Kriz GS (2001) Introduction to spectroscopy. (3rd edn) Thomson Learning, Singapore.
24. Ulutas K, Deger D, Kalkan N, Yildirim S, Celebi YG, et al. (2010) Structural properties of In-In₂O₃ composite films. IOP Conf Series: Mater Sci Eng 15: 012095.
25. Schwertmann U, Cornell RM (2008) Iron Oxides in the Laboratory: Preparation and Characterization. John Wiley & Sons.
26. Inoue M, Hirasawa I (2013) The relationship between crystal morphology and XRD peak intensity on CaSO₄•2H₂O. J Cryst Growth 380: 169-175.
27. Dhabade VV, Tallapragada RM, Trivedi MK (2009) Effect of external energy on atomic, crystalline and powder characteristics of antimony and bismuth powders. Bull Mater Sci 32: 471-479.
28. Kumar P, Kar M (2014) Effect of structural transition on magnetic and dielectric properties of La and Mn co-substituted BiFeO₃ ceramics. Mater Chem Phys 148: 968-977.
29. Levitas VI, Henson BF, Smilowitz LB, Asay BW (2006) Solid-solid phase transformation *via* internal stress-induced virtual melting, significantly below the melting temperature. Application to HMX energetic crystal. J Phys Chem B 110: 10105-10119.
30. Padmavathi DA (2011) Potential energy curves & material properties. Mater Sci Applicat 2: 97-104.
31. Sharma HP, Srivastava Y (2010) National defence academy examination. Upkar Prakashan. India.
32. Middleton B, Phillips J, Thomas R, Stacey S (2012) Physics in Anaesthesia. Royal College of General Practitioners.
33. Liu G (2011) Synthesis, characterization of In₂O₃ nanocrystals and their photoluminescence property. Int J Electrochem Sci 6: 2162-2170.